RSM Modeling and Multi-Objective Optimization of Turning Parameters for Polyamide PA66 using PCA and PCA Coupled with TOPSIS

Ahmed ZAIDI, Septi BOUCHERIT, Mohamed AthmaneYALLESE, Salim BELHADI, Mounia KADDECHE

Mechanics and Structures Research Laboratory (LMS), Université 8 Mai 1945 Guelma BP 401 Guelma 24000, Algérie, E-mail: boucherit.sebti@univ-guelma.dz

Abbreviations

GFRP – glass fibre reinforced polyamide; PCD – polycrystalline diamond; CVD – diamond coated cutting tool; K15 – uncoated carbide tool; Vc – cutting speed; ap – cutting depth; f – feed speed; Q – material removal rate; Ra – arithmetic roughness; Ft – tangential cutting force; PCA – principal component analysis; TOPSIS – order preference by similarity to ideal solution; η – signal to noise ratio; Cor – correlation matrix; cov – covariance matrix; σ_{x_i} – normal deviation; λ_k – eigenvalue; V_{ik} – Eigenvector; PCs_i – principal component scores; PIS – positive ideal solution; NIS – negative ideal solution; C – closeness coefficient.

1. Introduction

Polymers have recently become the essential element of a vast number of everyday objects, in which they have often replaced natural substances. They are present in many industrial fields (automotive, aviation and robots....etc.) [1, 2, 3]. Molding and extrusion are the main ways that polymeric mechanical parts are made, unless they are made in small quantities, have complicated shapes, or need to have a good surface quality. Machining is now a necessity. During maintenance, it is often necessary to fix or change the size of mechanical parts made of plastic. This is because parts with specific shapes and very precise sizes can only be made using machining by material removal. Polyamide PA66 is one of the thermoplastic polymers. It is used especially in the manufacture of automobile structural parts, in industrial gears such as marine propellers ...etc. The latter cause difficulties when cutting due to their special features such as low modulus of elasticity, moisture absorption rate, high coefficient of thermal expansion and internal stresses. In machining, the chemical and physical properties of polymeric materials have a significantly greater impact. Due to their viscoelastic behavior, it is difficult to figure out the connection between machinability and material qualities because of their viscoelastic behavior [4]. Turning has made considerable progress in the last few decades and enable easier machining of difficult-to-cut materials and greater machinability (better surface smoothness and lower cutting forces) [5].

Unfortunately, the same qualities that make it one of the foremost important engineering materials also lead to poor machinability resulting in short tool life, poor surface quality, high power consumption and, consequently, high cost [6], for these reasons that have led many researchers to carry out various studies with the aim of optimizing the machinability of these polymers. Davim and Silva [7] studied

PA66- GF30 and PA66 machinability during precision turning. They tested several values of feed rates and used four different tool materials. Results confirmed that radial force component have the highest values, followed by cutting and feed forces. The PCD tool delivered the most reduced force values that are in connection with the best surface quality, followed by the K15 grade uncoated carbide tool with chip breaker while machining reinforced polyamide. Continual winding of the chip was obtained, with all different parameters and tool materials used. Tezel [8] investigated the impact of manufacturing parameters together with machining allowance and tool feed on the quality of the hole surface and dimensional accuracy on a polyamide part shaped with a three-dimensional printer, was drilled and rubbed in a CNC machine. It has been proven that the surface quality of the holes in the polyamide material is straightforwardly depends on the machining allowance and an increment in the feed rate because of each manufacturing processes. Furthermore, the holes produced by the 3D printer are of poor quality, and rubbing is definitely required. Davim and Mata [9] evaluated the influence of glass fibre reinforcement during the turning of PA66 and PA66-GF30 polymers using a cemented carbide tool (K15). The authors found that the presence of glass fibres in PA66-GF30 polymer leads to higher values of cutting forces. Fountas et al [10] utilized cemented carbide cutting tools in turning composite PA66-GF30 at various Vc and f, using Soft Computing Techniques to examine experimentally and theoretically the impact of the glass fiber reinforcement on different cutting forces components Ft, Fv and Fr. According the findings, f incorporates a substantial impact on the outputs process. In longitudinal turning, the percentages of measured responses exceeded 80%, this explains that low values of f allow for a consistent machining. Vc has a less impact on observable responses and, in comparison to f. It gives lower cutting forces when utilized at low levels. The proposed software calculation techniques were also proven to be able of estimating cutting force components, thus improving decision making during planning machining process by avoiding costly use and time-consuming techniques. Davim and Mata [11], examined the machinability of two types of cutting tools used for turning GFRP composites (polycrystalline diamond PCD and cemented carbide tool K15). The machinability was assessed based on the value of the machinability index that they established. The research revealed that the PCD tool has a higher machinability index than the K15. Therefore, the PCD cutting tool provided the best overall performance. Silva [12] investigated the effects of polycrystalline diamond (PCD), CVD diamond coated carbide, and plain cemented carbide tools (K15-KF and

K15) on micro-turning PA66-GF30 under various cutting circumstances. The tools with the best results were the PCD tool, followed by the uncoated carbide inserts and the CVD diamond coated carbide tool. The tools with the best results had the smallest edge radius. Palani Kumar[13, 14] optimized the process parameters using the Taguchi approach of experimental layout, ensuing in low tool wear. Many researchers in various scientific domains, employ the Principal Component Analysis (PCA) and also in the field of mechanical manufacturing and especially in diverse machining processes. In recent years, PCA appears to be a broadly utilized analysis tool for process optimization with several performance characteristics [15]. Kavimani et al [16], Ray [17] have successfully utilized the PCA approach in electrical discharge machining. Viswanathan et al [18], Umamaheswarrao et al [19], Ananthakumar et al [20] have also applied it to optimize the cutting conditions in turning. Also, other researchers have utilized this approach to optimize the operating parameters in distinct machining processes like drilling and milling [21-23].

On the alternative hand, the Order Preference by Similarity to Ideal Solution (TOPSIS) technique is frequently used to solve multi-response optimization issues, such as determining the perfect combination of cutting parameters while machining diverse materials [24-26].

The goal of this research is to first determine how cutting parameters and their interactions influence the responses acquired during the turning process. In the second step, the output parameters of arithmetic roughness Ra and cutting force Ft are modeled using a Taguchi factorial design L_{27} and Response Surface Methodology (RSM). The current study's final stage is multi-objective optimization using two approaches. The first is PCA, while the second is PCA in conjunction with TOPSIS. The results of the optimization are then compared to the responses given by the total desirability function for the two ideal cutting regimes.

2. Experimental procedures

2.1. Material, workpiece and tool

For the various machining operations, a typical lathe from the Czech manufacturer "TOS TRENCIN" model SN40C SPINDLE with a power of 6.6 kW was utilized. The material used is polyamide PA66. It's a popular alternative to bronze, aluminium, and other non-ferrous metals for general-purpose wear and structural elements that require a good mixture of strength and toughness. PA66 has good mechanical and electrical properties such as insulation, good toughness, good abrasion and shock resistance, vibration dampers, high fatigue resistance, as it has significant weight benefits of 1.15 g/cm³ over bronze 8.8 g/cm³, which makes the comparative volume price very attractive. PA66 pulleys, gears, vibration dampers, and other structural parts are used in a variety of applications.

Fig. 1 Polyamide workpiece

Rods with a diameter of 90 mm and several grooves at a distance of 20 mm were used as test specimens (Fig. 1). Table 1 lists the physical and mechanical properties of PA66. The carbide insert SPMR 120308 was used for all turning operations. The cutting insert is mounted on a positive cutting angle tool holder labeled CSDPN 25X25M12.

Table1

Physical properties of PA66

Properties	Values
Density	1.15 g/cm3
Absorption of moisture (by weight)	8 %
Resistance tensile	80 MPa
Module elasticity tensile	3000 MPa
Melting temperature	220 C°
thermal conductivity	0.23 W/(m*k)

2.2. Measuring instruments

The mean values of the cutting force components Fa, Fr and Ft were measured with a platform (KISTLER Type 9257A). The recorded force signals were analyzed on machined lengths of 20 mm. The criterion Ra was obtained from a Mitutoyo Surftest 201 roughness meter as shown in Fig. 2. Measurements were repeated at three equally spaced locations around the perimeter of the part at 120° and attempted to average these values. The surface roughness was measured directly on the part without dismantling the lathe to reduce measurement errors. The setup arrangement is illustrated in Fig. 3.

Fig. 2 Roughness measurement

2.3. Experiments design

The studies used the conventional orthogonal table L_{27}Taguchi, which has 27 rows corresponding to the number of tests (26 degrees of freedom) and 13 columns at three levels [27]. The parameter levels chosen are as follows: Vc (200, 280 and 380) m/min, f (0.08, 0.16 and 0.24) mm/rev, and ap (1, 1.5 and 2) mm. Those levels are selected from the recommended ranges of the cutting tool manufacturer.

Table 2 shows all responses to the following factors: Ft, Ra and Q. The aim is to analyse the influence of various cutting parameters ap, Vc, f on the above output responses according to a Taguchi plan L_{27}. Q (cm³/min) was calculated based on Eq. (1).

$$Q\left[\text{cm}^3/\text{min}\right] = Vc \times f \times ap. \tag{1}$$

2.4. Statistical analysis methods

The statistical analysis of the results was carried

out in three parts: Using the ANOVA approach, the main effects of the factors and their interactions are analysed in the first section. The second method is quadratic regression, which is used to build analytical models that demonstrate output variance. The RSM was also used to build a link between machining settings and process characteristics [28, 29]. Finally, to improve the processing settings, a method called PCA and, secondly, a PCA-TOPSIS were utilized, which is a useful tool for optimizing multiple response problems [30].

3. Results and discussion

3.1. ANOVA and effects of factors

ANOVA is a combination of statistical models used to analyse differences between group means in a sample. It was used to determine whether cutting parameters had a substantial impact on output parameters [31, 32].

Table 3 illustrate the ANOVA results for Ft, and Ra, respectively, for a 95% confidence level. These tables show the DF values, the sum of the squares of the deviations (SS), the mean square (MS), and the percentage contribution (cont. %) of each model term are listed.

From the analysis of Table 3, a we can notice that f is the main factor influencing Ft, followed by ap, then the interaction $f*ap$, whose contributions are sequentially 46.28%, 39.96% and 7 .38% of the model, the other factors are considered insignificant. The same trend of results has been reported by Lazarevic et al. [33] when turning PA66 and Suhail et al. [34] in turning of Polytetrafluoroethylene.

The ANOVA of Ra is presented in Table 3, b where we can also state that f is the most important factor influencing Ra at 68.49% of the contribution. The second important term affecting Ra is Vc with 18.69% of the contribution, and f^2 with 8.25% followed by Vc^2 with 1.6%. The other terms can be assumed to be insignificant. This can be explained by the combined movement between the rotational movement of the workpiece and the translation of the tool, which forms a helical track of the tool around the workpiece. Similar results were published by Jiang et al. [35], Kini et al. [36], on turning various polymers.

3.2. Modelling development using RSM

The RSM is a mathematical-statistical technique that is widely used in modelling and analyzing many problems when a response of interest is influenced by several variables and the goal is to optimize that response [37].

Generally, in RSM problems, the relationship between the input and the output variables is expressed by the fully quadratic model. this model was used to obtain models which are useful for predicting response parameters against input control parameters [38]. The model can be explained as Eq. (2):

$$Y = a_0 + \sum_{i=1}^{n} a_{ii} X_i + \sum_{i=1}^{n} a_{ii} X_i^2 + \sum_{i \neq 1}^{n} a_{ij} X_i X_j, \qquad (2)$$

where: Y is the estimated response for Ft, and Ra; X_i is a factor influencing the response, corresponding to the studied cutting condition parameters such as Vc, f, ap and their interactions. Mathematical model coefficients a_0, a_{ii} and a_{ij} are assessed from the experimental results. These obtained models are given below by Eqs. (3) and (4).

The above models can be employed to predict the values of Ft, and Ra. Figs. 4, a-b illustrates the disparities between the quantified and predicted responses of Ra and Ft, respectively. The observed figures show that the predicted values of the various factors studied are closer to the experimentally recorded values; the findings of the comparison prove that quadratic models are efficient and capable of producing results comparable to experimental results.

3.3. 3D Graphic analysis

To investigate the influence of variable interaction on the response factors, 3D surfaces and contour diagrams were produced based on the model equations (Eqs. (2) and (3)) in Figs. 5 and 6 respectively. The 3D response surface plots were generated simultaneously considering two processing parameters, with the last variable for each diagram being kept constant on the middle plane.

Table 2

Experimental results for responses factors

Input cutting parameters			Output collect data		Calculated factors
Vc, m/min	F, mm/rev	ap, mm	Ft, N	Ra, μm	Q, cm³/min
200	0.08	1	32.11	2.73	16.00
		1.5	35.42	2.78	24.00
		2	37.28	2.57	32.00
	0.16	1	43.13	2.98	32.00
		1.5	59.77	2.91	48.00
		2	65.88	2.69	64.00
	0.24	1	43.34	4.41	48.00
		1.5	74.27	4.06	72.00
		2	95.98	4.49	96.00
280	0.08	1	25.53	2.74	22.40
		1.5	30.37	2.57	33.60
		2	45.88	2.19	44.80
	0.16	1	35.05	2.93	44.80
		1.5	74.43	2.66	67.20
		2	76.89	2.66	89.60
	0.24	1	50.17	4.29	67.20
		1.5	82.69	4.08	100.80
		2	105.81	4.23	134.40
380	0.08	1	22.46	1.36	30.40

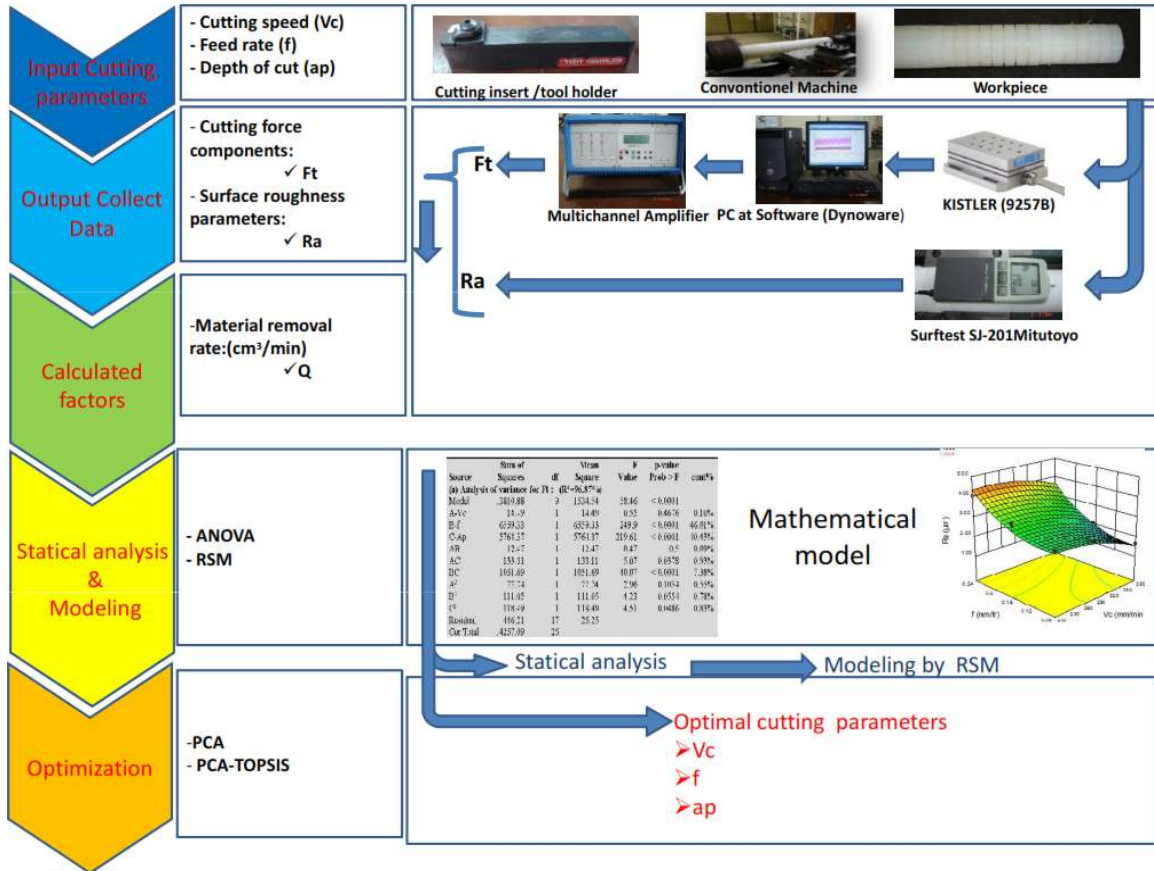| Input cutting parameters			Output collect data		Calculated factors
Vc, m/min	F, mm/rev	ap, mm	Ft, N	Ra, µm	Q, cm³/min
		1.5	42.52	1.65	45.60
		2	48.98	1.39	60.80
		1	37.47	2.11	60.80
	0.16	1.5	62.28	2.09	91.20
		2	76.69	2.15	121.60
		1	43.07	3.35	91.20
	0.24	1.5	70.69	3.51	136.80
		2	99.17	3.77	182.40

Fig. 3 Diagram of the experimental steps and modelling procedure

Table 3

ANOVA for output factors: a) Ft; b) Ra

Source	DF	Seq SS	Adj SS	Adj MS	F-Value	P-Value	Cont %	Remarks
a) Analysis of variance for Ft: R^2 = 96.87 %								
Model	9	13810	13810	1534	58.46	0	96.87	S
Linear	3	12306	12338	4112	156.6	0	86.32	S
Vc	1	10.6	14.5	14.49	0.55	0.468	0.07	NS
f	1	6598.7	6559	6559	249.9	0	46.28	S
ap	1	5697	5764	5764	219.6	0	39.96	S
Square	3	307.3	307.3	102.4	3.9	0.027	2.16	S
$Vc*Vc$	1	77.7	77.7	77.74	2.96	0.103	0.55	NS
$f*f$	1	111.1	111.1	111.0	4.23	0.055	0.78	NS
$ap*ap$	1	118.5	118.5	118.4	4.51	0.049	0.83	S
Interaction	3	1197.	1197.	399.0	15.2	0	8.40	S
$Vc*f$	1	12.5	12.5	12.47	0.47	0.5	0.09	NS
$Vc*ap$	1	133.1	133.1	133.1	5.07	0.038	0.93	S
$f*ap$	1	1051	1051	1051	40.07	0	7.38	S
Error	17	446.2	446.2	26.25			3.13	
Total	26	1425					100.0	
b) Analysis of variance Ra: R^2 = 98.51 %								
Model	9	21.75	21.75	2.417	124.6	0	98.51	S
Linear	3	19.26	19.18	6.393	329.7	0	87.23	S

Source	DF	Seq SS	Adj SS	Adj MS	*F-Value*	*P-Value*	Cont %	Remarks
Vc	1	4.127	3.957	3.957	204.1	0	18.69	S
f	1	15.12	15.21	15.21	784.7	0	68.49	S
ap	1	0.011	0.008	0.008	0.44	0.517	0.05	NS
Square	3	2.190	2.190	0.730	37.65	0	9.92	S
*Vc*Vc*	1	0.3542	0.354	0.354	18.27	0.001	1.60	S
*f*f*	1	1.822	1.822	1.822	93.99	0	8.25	S
*ap*ap*	1	0.013	0.013	0.013	0.71	0.412	0.06	NS
Interaction	3	0.300	0.300	0.100	5.16	0.01	1.36	S
*Vc*f*	1	0.116	0.116	0.116	6.01	0.025	0.53	S
*Vc*ap*	1	0.127	0.127	0.127	6.59	0.02	0.58	S
*f*ap*	1	0.056	0.056	0.056	2.89	0.107	0.25	NS
Error	17	0.329	0.329	0.019			1.49	
Total	26	22.08					100	

S: Significant; NS: Not significant

$$Ft[N] = -43.7164 + 0.1833.Vc + 143.878.f + 30.2881.ap - 0.1413.Vc.f + 0.0739.Vc.ap + 234.042.f.ap -$$
$$-0.0004.Vc^2 - 672.222.f^2 - 17.7756.ap^2, \tag{3}$$

$$Ra[\mu m] = 4.5411 + 0.0068.Vc - 22.5735.f - 1.5537.ap + 0.0137.Vc.f + 0.0023.Vc.ap + 1.7084.f.ap -$$
$$-0.00003.Vc^2 + 86.1111.f^2 + 0.1911.ap^2. \tag{4}$$

Fig. 5, a and b show that the effect of *Vc* on *Ft* is not significant compared to f and *ap*. Increases in *f* and *ap* clearly result in a considerable rise in *Ft*, which is attributable to the increased cross-sectional area of the cutter excised [27]. It is also worth noticing that the factor *f* slope is slightly higher than that of *ap* (Fig. 5, c). On the other hand, *Ft* falls when *Vc* rises because the temperature in the cutting plane area rises, making polyamide machining easier. Fig. 6 shows the interaction effects of *ap*, *f* and *Vc* on the *Ra*, Fig. 6, a and b show a negligible effect of *Vc* on *Ra* compared to the effects of *f* and *ap*. Fig. 6, c shows that increasing *f* and ap leads to an increase in *Ra*. However, it is noted that the effect of *f* is more marked, as demonstrated by [39] during the turning of the different polymers.

3.4. Optimization of cutting conditions

Quality and productivity are the really important properties of interest to all manufacturers, but these two criteria are inversely related, which is one of the greatest challenges for manufacturers. Various approaches have been proposed to resolve this problem. The PCA is a multivariate data analysis that was introduced by Pearsion [39]. It is currently the most generally utilized methods for reducing knowledge and interpreting multi-objective data sets. Recently, many researchers [40, 41] have proved that TOPSIS coupled with PCA can excellently be employed to work out the simplest combinations of turning factors thus allowing for optimal machining performance.

3.4.1. PCA method

To analyse the data using Principal Component Analysis (PCA) we adopted the following step research methodology.
Step 1. Compute the Taguchi's signal-to-noise (S/N) ratios for all output response. This ratio η_{ij} is classified into two categories in agreement to the objective target [42].
-    Lower-The-Better (LTB):

$$\eta_{ij} = -10\log_{10}\left(\frac{1}{n}\sum_{k=1}^{n} y_{ijk}^2\right). \tag{5}$$

-    Higher-The-Better (HTB):

$$\eta_{ij} = -10log_{10}\left(\frac{1}{n}\sum_{k=1}^{n}\frac{1}{y_{ijk}^2}\right), \tag{6}$$

where: y_{ijk} is the gauged response n is the number of repeated experiments.
Step 2. The array of correlation coefficients can be evaluated as:

$$Cor_{jl} = \frac{cov(\eta_i(j), \eta_i(l))}{\sigma_{x_i}(j) \times \sigma_{x_i}(l)} \quad j = 1, 2, ..., m; \ l = 1, 2, ..., n, \tag{7}$$

where: $cov(\eta_i(j), \eta_i(l))$ is the covariance of the sequences $\eta_i(j)$ and $\eta_i(l)$, $\sigma_{x_i}(j)$ is the normal deviation of the quality characteristics.
The eigenvector and eigenvalues are assessed from the correlation coefficient array: $(Cor - \lambda_k I_m)V_{ik} = 0$, where λ_k is eigenvalues, and V_{ik} the eigenvectors relate to the eigenvalues.
Step 3. Find the corresponding principal components of the quality characteristics that can be obtained using Eq. (8):

$$PCs_i(k) = \sum_{j=1}^{m} \eta_i(j)V_{ij} \ ; i = 1; 2, ..., n; \ j = 1, 2, ..., m. \tag{8}$$

Step 4. Choose components that have about 80% of the variance explained to build the multiple performance index *MPI*: $MPI_i = \sum_{j=1}^{m}\frac{\lambda_j}{\sum_{j=1}^{m}\lambda_j} \times PCs_i(j)$.

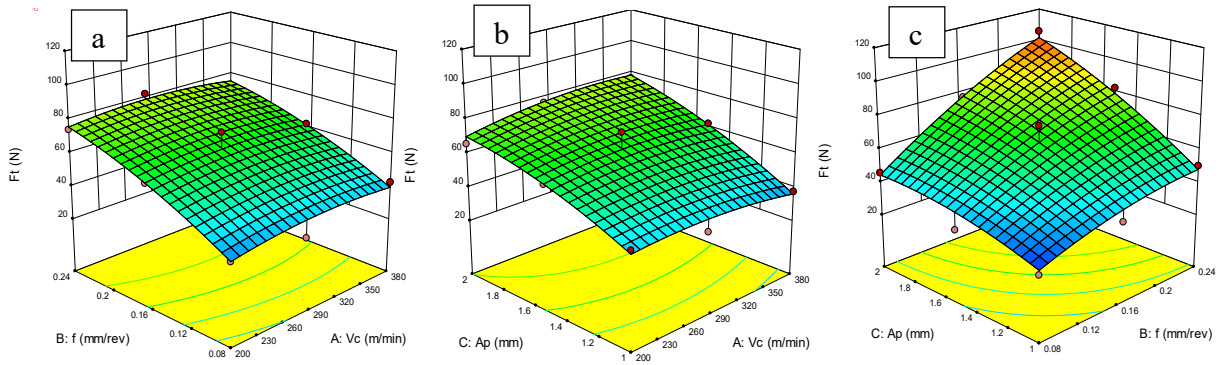**Step 5.** Rank the MPIs. The best solution to the optimization issue correlates to the highest rank.

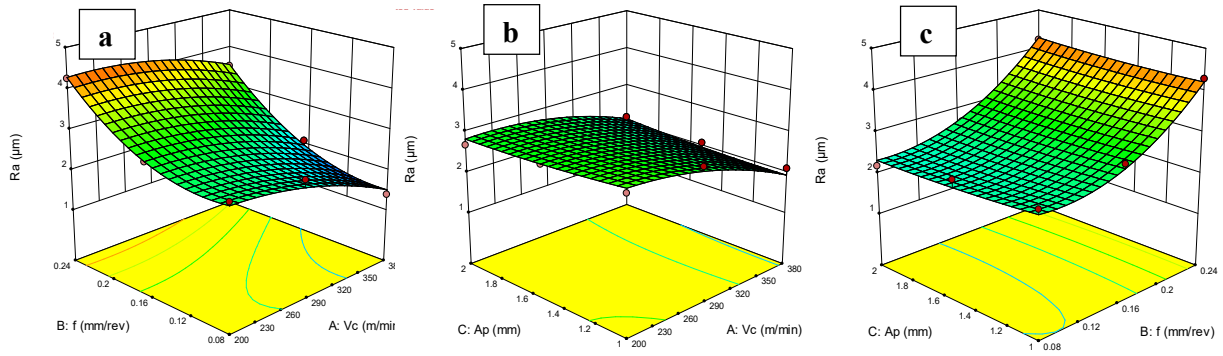Fig. 5 Estimated responses surface of *Ft* versus *Vc*, *f* and *ap*

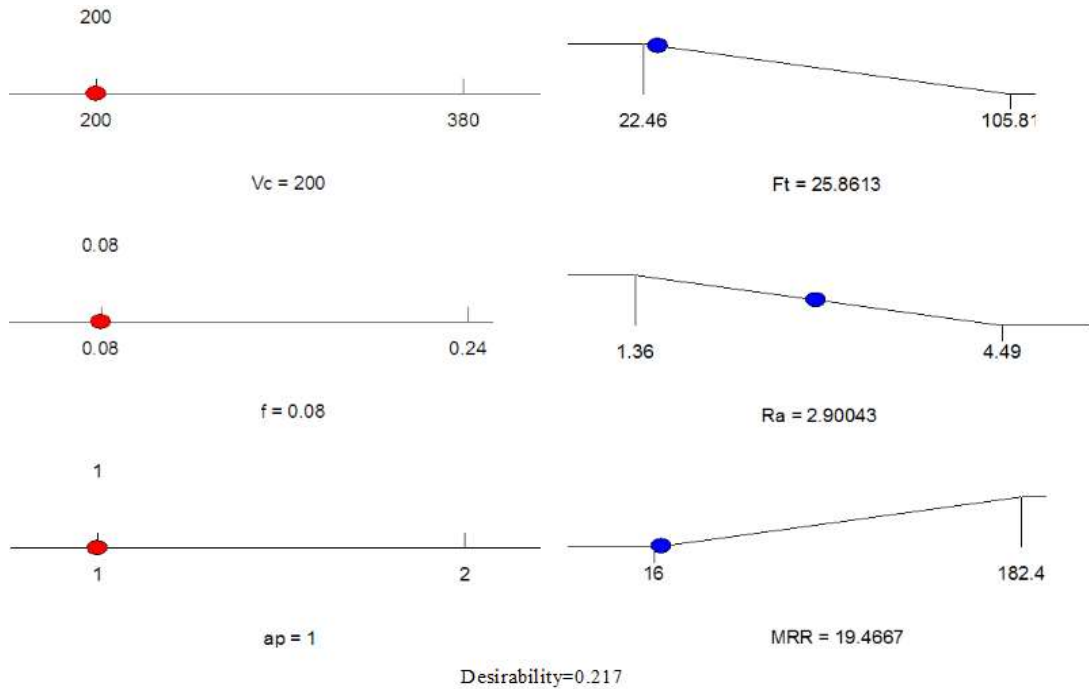Fig. 6 Estimated responses surface of *Ra* versus *Vc*, *f* and *ap*

Fig. 7 Ramp function graph (PCA Solution)

3.4.2. PCA based TOPSIS Method

In order to carry out the optimization through principal component analysis coupled with the TOPSIS method, we adopt identical steps as described above up to step 3, and then we have to proceed as follows:

Step 1. The following Eq. (9) would be applied to normalize the performing decision matrix:

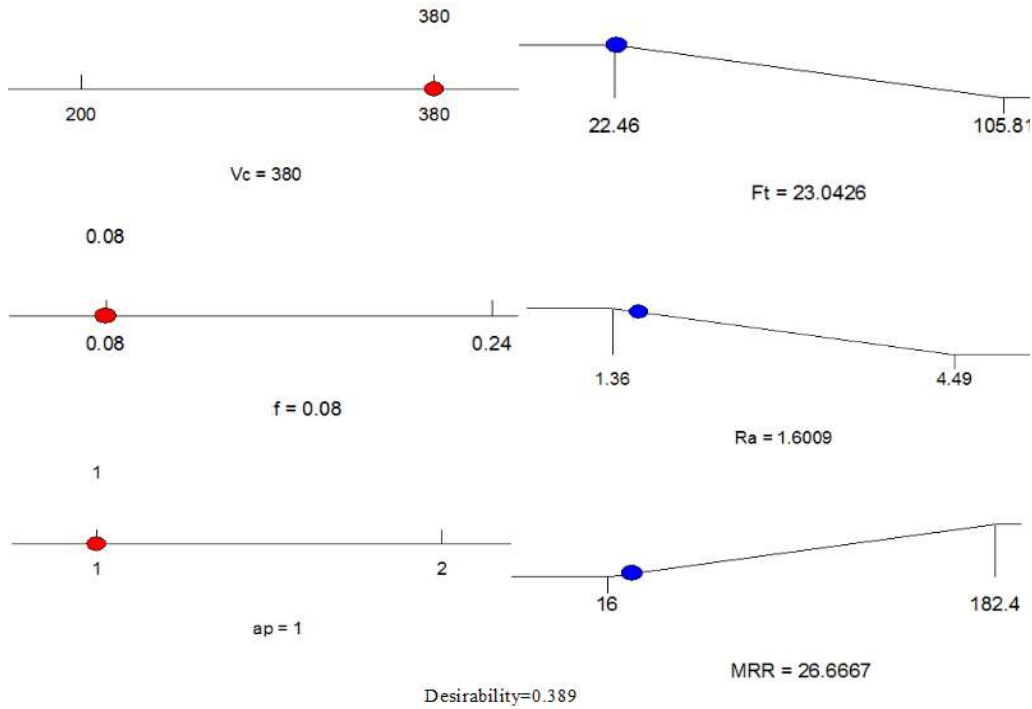$$r_i(k) = \frac{PCs_i(k)}{\sqrt{\sum_{i=1}^{m} PCs_i(k)^2}}. \qquad (9)$$

Fig. 8 Ramp function graph (PCA-TOPSIS Solution)

Step 2. Calculate the weighted normalized Matrix as follow:

$$P_i(k) = \lambda_i \times r_i(k), \tag{10}$$

where: λ_i are the weights (i.e. eigenvalues connected with each principal component); $P_i(k)$ was the weighted quality performance matrix.

Step 3. Ascertain the Positive Ideal Solution (*PIS*) and Negative Ideal Solution (*NIS*) in the following manner:

$$PIS = (pis_1, pis_2, ..., pis_n) \text{ Maximum values}$$
$$NIS = (nis_1, nis_2, ..., nis_n) \text{ Minimum values}. \tag{11}$$

Step 4. The separation of each alternative from *PIS* and *NIS* is determined as follows:

$$S^+(k) = \sqrt{\sum_{j=1}^{m}\left(P_i(k) - pis_j(k)\right)^2}, \tag{12}$$

$$S^-(k) = \sqrt{\sum_{j=1}^{m}\left(P_i(k) - nis_j(k)\right)^2}. \tag{13}$$

Step 5. Each alternative $C(k)$ closeness coefficient is quantified as:

$$C(k) = \frac{S^-(k)}{S^+(k) + S^-(k)}. \tag{14}$$

Step 6. Calculate the Rank. The optimum solution to the optimization issue correlates to the highest Rank.

3.4.3. Result of optimization

Three S/N ratios are used in this survey, namely, LTB for *Ra*, *Ft*, and HTB for *Q*. The S/N ratios for the five output responses are uncovered in Table 4. The resulting eigenvalues and the corresponding eigenvectors are uncovered in Table 5.

Table 4

Scaled S/N and PCs

S/N for *Ft*	S/N for *Ra*	S/N For *Q*	PC1	PC2	PC3
-30.1328	-8.7233	24.0824	-37.8091	3.8468	10.9414
-30.9850	-8.8809	27.6042	-41.1595	2.9067	9.9187
-31.4295	-8.1987	30.1030	-43.2749	1.4793	9.2907
-32.6956	-9.4843	30.1030	-44.2461	2.8411	9.9675
-35.5297	-9.2779	33.6248	-48.5942	1.8190	10.6937
-36.3751	-8.5950	36.1236	-50.9276	0.4431	10.3982
-32.7378	-12.8888	33.6248	-47.8699	4.8200	7.3317
-37.4163	-12.1705	37.1466	-53.1085	3.5606	9.7355
-39.6436	-13.0449	39.6454	-56.5358	3.8144	10.1341
-28.1410	-8.7550	27.0050	-39.0998	2.6241	7.8838
-29.6489	-8.1987	30.5268	-42.6497	1.1041	7.6119
-33.2325	-6.8089	33.0256	-46.3167	-0.5750	9.7916
-30.8938	-9.3374	33.0256	-45.6008	1.4766	7.1193
-37.4350	-8.4976	36.5474	-51.8258	0.3458	11.1026
-37.7174	-8.4976	39.0462	-54.0030	-0.4672	10.1424
-34.0089	-12.6491	36.5474	-50.8754	3.7680	7.0581
-38.3491	-12.2132	40.0692	-55.9921	2.7277	9.0994
-40.4905	-12.5268	42.5680	-59.2494	2.4480	9.5895
-27.0282	-2.6708	29.6575	-39.3050	-4.0892	7.4578
-32.5719	-4.3497	33.1793	-45.5412	-3.0035	9.8837
-33.8004	-2.8603	35.6781	-47.9055	-5.0810	10.1397
-31.4737	-6.4856	35.6781	-47.4373	-2.0062	7.1592
-35.8870	-6.4029	39.1999	-52.6715	-2.7081	9.1588
-37.6948	-6.6488	41.6987	-55.7324	-3.0941	9.3919
-32.6835	-10.5009	39.1999	-51.8304	0.6931	5.3143
-36.9872	-10.9061	42.7217	-57.1122	0.4316	7.0815
-39.9276	-11.5268	45.2205	-60.8715	0.5416	8.1449

<div style="columns:2">

Table 5

Eigenvalues, AP and Eigenvectors for PCs

	PC1	PC2	PC5
Eigenvalues	40.418	7.065	2.239
Accountability Proportion (AP)	81.3 %	14.2 %	4.5 %
Eigenvictors	0.544	-0.13	-0.829
	0.22	-0.931	0.29
	-0.81	-0.34	-0.478

The computed closeness coefficients of each alternative $C(k)$ of step 6 from the algorithm of PCA-TOPSIS are shown in Table 6.

Check the order of columns 3 and 5 in Table 6 to see which combination yields the desired outcome. The optimal factors levels are thus found using the criterion "the higher the rank value, the better." The levels at which the highest rank was reached correspond to alternatives N°1 for the PCA method and N°19 for the PCA-TOPSIS. i.e., $Vc = 200$ m/min, $f = 0.08$ mm/rev, $ap = 1$ mm. For PCA and $Vc = 380$ m/min, $f = 0.08$ mm/rev, $ap = 1$ mm, was found for PCA-TOPSIS. In order to deter-mine which of the two solutions offers the optimal cut-ting regime to meet the goals set previously, the total desirability function is used as a decision criterion. The graphical ramp function for the total desirability function of Ft, Ra, and Q is shown in Figs. 7 and 8. Fig. 7 shows the optimal solution given by PCA. Its desirability function value is 0.217, which is less than the optimal solution given by PCA-TOPSIS in Fig. 7, which is 0.389. This means that the second combination of the cutting regime is the best way to achieve the goals.

Table 6

PCA and PCA-TOPSIS results

Test N	PC1	Rank	PCA-TOPSIS	Rank
1	-30.7388	1	0.4494	13
2	-33.4626	4	0.4452	14
3	-35.1825	6	0.4873	9
4	-35.9721	7	0.4053	18
5	-39.5071	14	0.3880	19
6	-41.4041	16	0.4377	15
7	-38.9182	12	0.2826	22
8	-43.1772	20	0.2172	24
9	-45.9636	24	0.1370	27
10	-31.7881	2	0.4820	10
11	-34.6742	5	0.5172	8
12	-37.6555	10	0.5736	7
13	-37.0735	9	0.4554	11
14	-42.1343	17	0.4306	16
15	-43.9045	21	0.4536	12
16	-41.3617	15	0.2545	23
17	-45.5216	23	0.2117	25
18	-48.1697	26	0.1939	26
19	-31.9549	3	0.9093	1
20	-37.0250	8	0.7402	3
21	-38.9472	13	0.7698	2
22	-38.5666	11	0.6506	4
23	-42.8219	19	0.6027	5
24	-45.3104	22	0.5748	6
25	-42.1381	18	0.4097	17
26	-46.4322	25	0.3576	20
27	-49.4885	27	0.3187	21

4. Conclusions

In this experimental study, the focus was on modeling and determining the optimal cutting conditions for a desired surface quality with minimum cutting force and maximum turning productivity of polyamide PA66 was investigated. On the basis of the already discussed results, the following conclusions could be drawn:

1. The ANOVA results for Ra explain that feed rate is the most significant factor affecting Ra, followed by cutting speed while depth of cut has no effect on Ra, and their contributions are 68.49%; 18.69% and 0.05% respectively.

2. The ANOVA results for Ft explained that f is the most significant factor affecting Ft followed by ap, then the interaction of two factors ($f * ap$) their contributions are successively 46.28%, 39.96% and 7.38% of the model, and their contributions are 49.64, 22.06, and 19.65% respectively.

3. Optimization through PCA shows the optimal values on cutting parameters that leads to best surface quality, minimum cutting force and maximum Materiel removal rate are $Vc = 200$ m/min, $f = 0.08$ mm/rev, $ap = 1$mm. The optimized Ra, Ft and Q are as follows ($Ft = 32.11$N, $Ra = 2.73$μm, and $Q = 16$ cm^3/min).

4. The values of the optimal cutting parameters obtained with PCA-TOPSIS are as follows: $Vc = 380$ m/min, $f = 0.08$ mm/rev and $ap = 1$ mm. The optimized surface roughness and the material removal rate are as follows ($Ft = 22.46$N, $Ra = 1.36$μm, and $Q = 30.40$ cm^3/min).

5. The total desirability function offers an efficient way to compare different optimization methods.

Acknowledgements

References

1. **Deopura, B. L.; Alagirusamy, R.; Joshi, M.; Gupta, B.** 2008. Polyesters and polyamides, 2008th ed. Cambridge, England.

2. **Gaitonde, V. N.; Karnik, S. R.; Silva, L. R.; Abrão, A. M.; Davim, J. P.** 2009. Machinability study in micro Turning of PA66 GF30 polyamide with a PCD tool, Mater. Manuf. Process 24(12): 1290–1296. https://doi.org/10.1080/10426910903130115.

3. **Mata, F.; Reis, P.; Davim, J. P.** 2006. Physical cutting model of polyamide composites (PA66 GF30), Materials Science Forum 514-516: 643–647.

4. **Xiao, K. Q. and Zhang, L. C.** 2002. The role of viscous deformation in the machining of polymers, Int. J. Mech. Sci 44(11): 2317–2336. https://doi.org/10.1016/S0020-7403(02)00178-9.

5. **Vaxevanidis, N. M.; Kechagias, J. D.; Fountas, N. A.; Manolakos, D. E.** 2015. Evaluation of machinability in turning of engineering alloys by applying artificial neural networks, Open Constr. Build. Technol. J. 8(1): 389–399. https://doi.org/10.2174/1874836801408010389.

6. **Frifita, W.; Ben Salem, S.; Haddad, A.; Yallese, M. A.** 2020. Optimization of machining parameters in turning of Inconel 718 Nickel-base super alloy, Mech. Ind

</div>

21: 1-20.
https://doi.org/10.1051/meca/2020001.

7. **Davim, J. P.; Silva, L. R.; Festas, A.; Abrão, A. M.** 2009. Machinability study on precision turning of PA66 polyamide with and without glass fiber reinforcing, Mater. Des 30(2): 228–234.
https://doi.org/doi: 10.1016/j.matdes.2008.05.003.

8. **Tezel, T**. 2020. Comparison of hole quality of polyamide materials produced by traditional and additive manufacturing, International Journal of Advances in Engineering and Pure Sciences 32(1): 1-7.

9. **Davim, J. P.; Mata, F.** 2007. A comparative evaluation of the turning of reinforced and unreinforced polyamide, Int. J. Adv. Manuf. Technol. 33(9-10): 911–914.

10. **Fountas, N. A.; Ntziantzias, I.; Kechagias, J.; Koutsomichalis, A.; Davim, J. P.; Vaxevanidis, N. M.** 2013. Prediction of cutting forces during turning PA66 GF-30 glass fiber reinforced polyamide by soft computing techniques, Mater. Sci. Forum 766: 37–8.
https://doi.org/0.4028/www.scientific.net/MSF.766.37.

11. **Davim, J. P.; Mata, F.** 2007. New machinability study of glass fibre reinforced plastics using polycrystalline diamond and cemented carbide (K15) tools, Mater. Des 28(3): 1050–1054.
https://doi.org/10.1016/j.matdes.2005.09.019

12. **Silva, L. R.; Davim, J. P.; Festas, A.; Abrão, A. M.** 2009. Machinability aspects concerning micro-turning of PA66-GF30-reinforced polyamide, Int. J. Adv. Manuf. Technol. 41: 839–845.
https://doi.org/10.1007/s00170-008-1537-y.

13. **Palanikumar, K.** 2008. Application of Taguchi and response surface methodologies for surface roughness in machining glass fiber reinforced plastics by PCD tooling, Int. J. Adv. Manuf. Technol. 36(1–2): 19–27.

14. **Palanikumar, K.; Karunamoorthy, L.; Karthikeyan, R.** 2004. Optimizing the machining parameters for minimum surface roughness in turning of GFRP composites using design of experiments, Journal of Materials Science and Technology Shenyang 20(4): 373-378.

15. **Caggiano, A.** 2018. Tool wear prediction in Ti-6Al-4V machining through multiple sensor monitoring and PCA features pattern recognition, Sensors 18(3): 823.
https://doi.org/10.3390/s18030823.

16. **Kavimani, V.; Prakash, K. S.; Thankachan, T, Nagaraja, S.; Jeevanantham, A. K; Jhon, J. P.** 2020. WEDM parameter optimization for silicon@ r-GO/magneisum composite using taguchi based GRA coupled PCA, Silicon 12(5): 1161-1175.
https://doi.org/10.1007/s12633-019-00205-6.

17. **Ray, A.** 2016. Optimization of process parameters of green electrical discharge machining using principal component analysis (PCA), Int. J. Adv. Manuf. Technol. 87: 1299–1311.
https://doi.org/10.1007/s00170-014-6372-8.

18. **Viswanathan, R., Ramesh, S., Maniraj, S., Subburam, V.** 2020. Measurement and multi-response optimization of turning parameters for magnesium alloy using hybrid combination of Taguchi-GRA-PCA technique, Measurement 159: 107800.
https://doi.org/10.1016/j.measurement.2020.107800.

19. **Umamaheswarrao, P.; Raju, D. R.; Suman, K. N. S.; Sankar, B. R**. 2018. Multi objective optimization of process parameters for hard turning of AISI 52100 steel using Hybrid GRA-PCA, Procedia computer science 133: 703-710.

20. **Ananthakumar, P.; Ramesh, M.** 2013. Optimization of turning process parameters using multivariate statistical method-PCA coupled with Taguchi method, International Journal of Scientific Engineering and Technology 2(4): 263-267.

21. **Kharwar, P. K.; Verma, R. K.** 2020. Machining performance optimization in drilling of multiwall carbon nano tube/epoxy nanocomposites using GRA-PCA hybrid approach, Measurement 158: 107701.

22. **Qazi, M. I.; Abas, M.; Khan, R; Saleem, W.; Pruncu, C. I.; Omair, M.** 2021. Experimental investigation and multi-response optimization of machinability of AA5005H34 using composite desirability coupled with PCA, Metals 11(2): 235.

23. **Bhosale, S. B.; Bhowmik, S.; Ray, A**. 2021. Experimental analysis and parametric optimization of drilling process for ferrous clay composite using GRA-PCA approach, Journal of Materials Research and Technology 10: 376-389.
https://doi.org/10.1016/j.jmrt.2020.12.032.

24. **Singaravel, B.; and Selvaraj, T.** 2015. Optimization of machining parameters in turning operation using combined TOPSIS and AHP method, Tehnicki Vjesnik 22(6): 1475-1480.
https://doi.org/10.17559/TV-20140530140610.

25. **Abbas, A. T.; Sharma, N.; Anwar, S.; Luqman, M.; Tomaz, I.; Hegab, H.** 2020. Multi-response optimization in high-speed machining of Ti-6Al-4V using TOPSIS-fuzzy integrated approach, Materials 13(5): 1104.
https://doi.org/10.3390/ma13051104.

26. **Huu Phan, N.; Muthuramalingam, T.** 2021. Multi-criteria decision-making of vibration-aided machining for high silicon-carbon tool steelwith Taguchi–topsis approach, Silicon 13(8): 2771-2783.
https://doi.org/10.1007/s12633-020-00632-w.

27. **Chabbi, A.; Yallese, M. A.; Nouioua, M.; Meddour, I.; Mabrouki, T.; Girardin, F.** 2017. Modeling and optimization of turning process parameters during the cutting of polymer (POM C) based on RSM, ANN, and DF methods, Int. J. Adv. Manuf. Technol. 91(5–8): 2267–2290.
https://doi.org/10.1007/s00170-016-9858-8.

28. **Aultrin, K. J.; Anand, M. D**. 2016. Experimental investigations and prediction on MRR and SR of some non ferrous alloys in AWJM using ANFIS, Indian J. Sci. Technol. 9(13): 1-21.
https://doi.org/10.17485/ijst/2016/v9i13/90585.

29. **Kolahan, F.; Khajavi, A. H.** 2009. A statistical approach for predicting and optimizing depth of cut in AWJ machining for 6063-T6 Al alloy, International Journal of Mechanical and Mechatronics Engineering 3(11): 1395-1398.
https://doi.org/10.5281/zenodo.1078176.

30. **Naveen Sait, A.; Aravindan, S.; Noorul Haq, A.** 2009. Optimisation of machining parameters of glass-fibre-reinforced plastic (GFRP) pipes by desirability function analysis using Taguchi technique, Int. J. Adv. Manuf. Technol. 43(5–6): 581–589.

31. **Camposeco-Negrete, C.** 2013. Optimization of cutting parameters for minimizing energy consumption in turning of AISI 6061 T6 using Taguchi methodology and ANOVA, J. Clean. Prod. 53: 195–203.

https://doi.org/10.1016/j.jclepro.03.049.

32. **Bouzid, L.; Boutabba, S.; Yallese, M. A.; Belhadi, S.; Girardin, F.** 2014. Simultaneous optimization of surface roughness and material removal rate for turning of X20Cr13 stainless steel, Int. J. Adv. Manuf. Technol. 74(5–8): 879–891.

33. **Lazarevic, D; Madic, M; Jankovic, P.; Lazarevic, A.** 2012. Surface roughness minimization of polyamide PA-6 turning by Taguchi method, Journal of Production Engineering 15(1): 29–32.

34. **Suhail, M.; Deepak, A.; Nikam, S.** 2014. Study of cutting forces and surface roughness in turning of bronze filled polytetrafluoroethylene,Int. J. Adv. Mech. Eng. 4(2): 151–160.

35. **Jiang, Q.; Zhang, L. C.; Pittolo, M.** 2000. The dependence of surface finish of a spectacle polymer upon machining conditions, Prog. Mach. Technol. Aviat. Ind. Press. Beijing, pp. 7–12.

36. **Kini, M. V.; Chincholkar, A. M.** 2010. Effect of machining parameters on surface roughness and material removal rate in finish turning of ±30° glass fibre reinforced polymer pipes, Mater. Des 31(7): 3590–3598. https://doi.org/10.1016/j.matdes.2010.01.013.

37. **Khuri, A. I.; Mukhopadhyay, S.** 2010. Response surface methodology,Wiley Interdiscip. Rev. Comput. Stat. 2(2): 128–149.

38. **Keblouti, O.; Boulanouar, L.; Azizi, M. W.; Yallese, M. A.** 2017. Effects of coating material and cutting parameters on the surface roughness and cutting forces in dry turning of AISI 52100 steel, Struct. Eng. Mech. 61(4): 519–526.
https://doi.org/10.12989/sem.2017.61.4.519.

39. **Pearson, K.** 1901 On lines and planes of closest fit to systems of points in spaces, Philos Mag. Ser. 62: 559–572.

40. **Hwang, CL.; dan Yoon K.** 1981. Multiple Attribute Decision Making-Methods and Applications, A State of the Art Survey. New York: Springer-Verlag.

41. **Rahmasari, F.; Indahwati, S.; Utamin, S.** 2017. Optimization multiple responses of Taguchi method using PCA- TOPSIS and VIKOR method, International Journal of Scientific & Engineering Research 8(2): 404-407.

42. **Taguchi, G.** 1986. Introduction to quality engineering. Asian Productivity Organization, UNIPUB, New York.

A. Zaidi, S. Boucherit, M. A. Yallese, S. Belhadi, M. Kaddeche

RSM MODELLING AND MULTI-OOBJECTIVE OPTIMIZATION OF TURNING PARAMETERS FOR POLYAMIDE (PA66) USING PCA AND PCA COUPLED WITH TOPSIS

S u m m a r y

In this study, turning operations on polyamide PA66 with a cemented carbide insert were organized according to the L_{27} Taguchi design, whose objective is the analysis of the cutting parameters on the output parameters (surface roughness and cutting force), as well as on the calculated parameter (material removal rate). The results revealed that surface roughness is highly impacted by the feed rate, which accounts for more than 68% of the variance, followed by the cutting speed, and finally the depth of cut. With respect to cutting force, depth of cut and feed rate have emerged as the most important terms. A mathematical model is then created to predict the surface roughness and cutting force. Finally, the optimal cutting regime leading to good surface quality with less cutting force and maximum productivity was examined using two multi-criteria optimization methods, namely PCA and PCA coupled with TOPSIS. The total desirability function was used as a decision criterion for evaluating the two optimization methods. The results demonstrate the potential superiority of the PCA-TOPSIS method over the PCA method.